Solid State and Electronic Structure of Rare Earth Metal Intercalated Graphite from First-principles Theory

Chang-Ming Fang, Joseph Bauer, Jean-Yves Saillard, and Jean-Francois Halet

Laboratoire des Sciences Chimiques de Rennes, UMR 6226 CNRS-Université de Rennes 1, Avenue du Général Leclerc, 35042 Rennes Cedex, France

Reprint requests to Dr. C.-M. Fang. E-mail: cm.fang@orange.nl
or Prof. Dr. J.-F. Halet. Fax: +33 2 23 23 68 40. E-mail: halet@univ-rennes1.fr

Z. Naturforsch. **2007**, *62b,* 971 – 976; received April 27, 2007

Dedicated to Dr. Bernard Chevalier on the occasion of his 60th birthday

The structural arrangements of the graphite intercalates LnC_6 (*Ln* = La, Ce, Nd and Yb) were investigated using Density Functional Theory (DFT) within the Generalized Gradient Approximation (GGA). The EuC_6-type structure ($A\alpha A\beta A\alpha A\beta A\alpha A$ stacking) is slightly energetically preferred for La and Ce, whereas with the other rare earth metals almost the same cohesive energies are found for the three different atomic arrangements $A\alpha A\alpha A\alpha A\alpha A\alpha A\ldots$, $A\alpha A\beta A\alpha A\beta A\alpha A\ldots$, and $A\alpha A\beta A\gamma A\alpha A\beta A\ldots$ A rather important charge transfer occurs from the metals to the carbon sheets, with the electrons partially occupying the bottom of the carbon π^* band. As a consequence, a lengthening of the C–C bond lengths of *ca*. 0.02 Å is computed with respect to the C–C bonds in graphite. Two-dimensional metallic character is expected for LaC_6 according to its band structure.

Key words: Intercalated Graphite, Density Functional Calculations, Electronic Structure, Rare Earth Metals, GIC's

Introduction

Numerous experimental and theoretical studies have been devoted over the years to graphite intercalation compounds (GIC's) due to the peculiar anisotropic structural, electronic, and transport properties of these materials [1 – 4]. GIC's consist of stacks of graphite layers alternating with layers of intercalated atoms or molecules. Weak van der Waals interactions between the graphite layers allow the incorporation of a wide variety of intercalants such as alkaline earth [2, 4 – 6] or rare earth metals [1, 3, 7]. Such an intercalation provides a means for controlling the physical properties of the graphite host. The free-electron concentration of graphite is very low and intercalation with different metals in different concentrations allows wide variations of the number of free electrons and thus of the electrical and magnetic properties.

Research on GIC's with rare earth metals (*Ln*), for instance, has recently undergone a resurgence of interest with the discovery of superconductivity in YbC_6 [7 – 11]. Rare earth metals are also promising candidates for magnetic GIC's [3, 7]. However, one of the limiting factors for an extensive study of *Ln* GIC's is the preparation of high-quality bulk samples for accurate structure determination [1, 7 – 12]. Carbide-contaminated SmC_6, EuC_6 and YbC_6 compounds were first made by interaction of graphite with rare earth metal vapour at 400 – 500 °C by Guérard and Hérold and their colleagues [12 – 14]. Later, Hagiwara *et al.* prepared new LnC_6 GIC's with *Ln* = Nd, Dy, and Er, as well as the previously reported ones (*Ln* = Eu, Sm, Yb) by interacting graphite and rare earth metals in molten chlorides below 400 °C [15]. *In situ* intercalation of La, Eu and Yb was achieved by Molodtsov *et al.* by deposition of the metals onto single-crystalline graphite (0001) substrates and subsequent annealing above 600 °C [16 – 18]. CeC_6 and NdC_6 powders were obtained from arc-melted samples in a search for new rare earth metal boron carbides [19].

Within the LnC_6 stoichiometry, intercalated rare earth metal atoms can be located in one of the three prismatic hexagonal sites denoted α, β, and γ. Assuming that all the graphite layers *A* stack in an eclipsed fashion, three different simple stacks can hypothetically be built, *i. e.*, $A\alpha A\alpha A\alpha A\alpha A\alpha A\ldots$, $A\alpha A\beta A\alpha A\beta A\alpha A\ldots$, and $A\alpha A\beta A\gamma A\alpha A\beta A\ldots$. The first and second stacks lead to hexagonal symmetry

0932–0776 / 07 / 0700–0971 $ 06.00

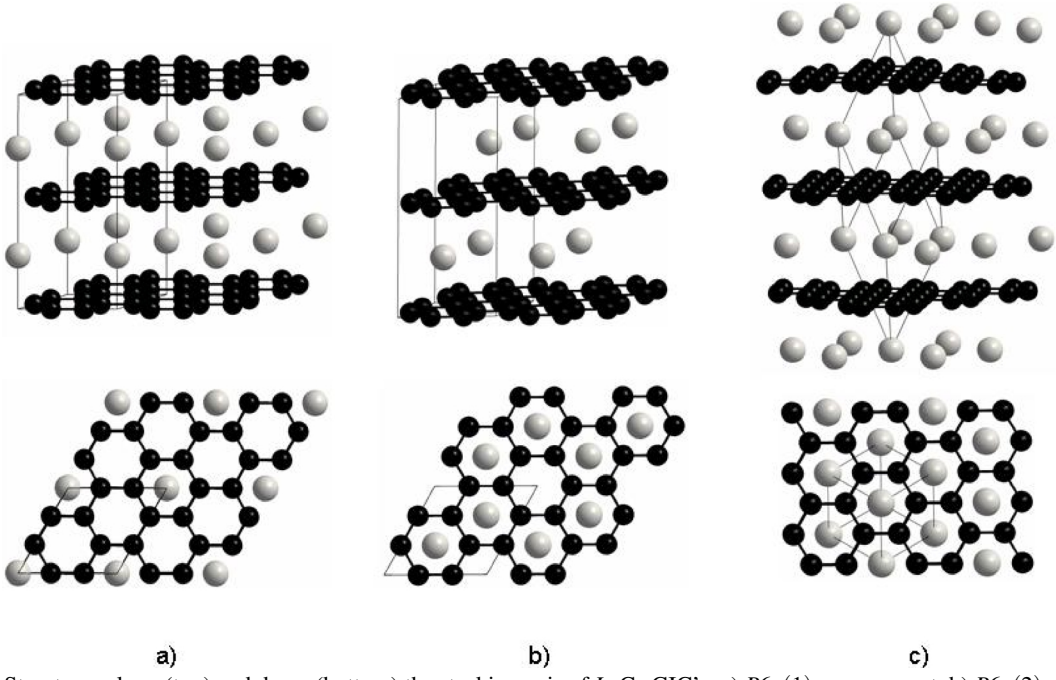

Fig. 1. Structures along (top) and down (bottom) the stacking axis of LnC_6 GIC's: a) $P6_3(1)$ arrangement, b) $P6_3(2)$ arrangement, c) $R3$ arrangement. Carbon and metal atoms are drawn as small black and large grey balls, respectively.

(both space group $P6_3/mmc$ with C at $12i$ (1/3,0,0) and *Ln* at $2c$ (1/3,2/3,1/4) for the former, and C at $12i$ (1/3,0,0) and *Ln* at $2b$ (0,0,1/4) for the latter), whereas the third one corresponds to rhombohedral symmetry (space group $R\bar{3}m$ with C at $6g$ $(x,-x,1/2)$ and *Ln* at $1a$ (0,0,0)). These arrangements, denoted $P6_3(1)$ ($A\alpha A\alpha A\alpha A\alpha A\alpha A$), $P6_3(2)$ ($A\alpha A\beta A\alpha A\beta A\alpha A$) and $R3$ ($A\alpha A\beta A\gamma A\alpha A\beta A$) in the following, are shown in Fig. 1. Most of the structural results reported so far seem to indicate that LnC_6 compounds adopt the hexagonal EuC_6-type structure $P6_3(2)$ [1, 3, 7, 12 – 17] (Fig. 1a). However, according to one of us, examination of the powder X-ray diffraction patterns of arc-melted NdC_6 and CeC_6 samples has led to a rhombohedral structure ($R3$) [19], similar to the crystal structure of CaC_6 newly determined by Emery *et al.* [4]. The arrangement $P6_3(1)$, observed for LiC_6 [12], has not been reported with rare earth metals as yet. Note that these experimental structural data must be discussed with caution. All the results were based on not very accurate powder diffraction patterns.

The few theoretical studies previously carried out on rare earth metal GIC's, sometimes accompanied with experimental photoemission measurements, mainly aimed at an understanding of the charge transfer from the metals to the graphite layers [10, 16, 17, 20] or the electron-phonon coupling in superconducting YbC_6 [10]. The relative stability of the three possible arrangements and their corresponding electronic structures have not been theoretically studied in detail as yet. A quantitative theoretical analysis at the Density-Functional Theory (DFT) level was thus carried out in order to gain further insight into the electronic factors (if any) contributing to the stability of one arrangement or another in these rare earth metal GIC's. The main results are reported in this paper.

Details of Theoretical Calculations

Total energy calculations were carried out using the first-principles molecular-dynamics computer code VASP (Vienna *ab initio* Simulation Program) [21, 22]. The calculations were carried out in the spin-polarized Generalized Gradient Approximation (SP-GGA) [23], using the projector-augmented wave (PAW) method [24, 25]. The electronic wave functions for the LnC_6 compounds considered were sampled on a $(12 \times 12 \times 8)$ and $(10 \times 10 \times 10)$ k point mesh in the Brillouin zone (BZ) corresponding to hexagonal or primitive rhombohedral cells, respectively [26]. The kinetic energy cut-off on the wave functions was set up at 800 eV,

Compound		$P6_3(1)$	$P6_3(2)$	$R3$
LaC_6	*E*	18	0	40
	a	4.333	4.338	4.333
	c	9.768	9.636	13.573
	d	4.884	4.818	4.524
	C–C (×3)	1.444	1.446	1.444
	La–C (×12)	2.84	2.81	2.68
CeC_6	*E*	53	0	68
	a	4.340	4.333	4.341 (*4.49*)[a]
	c	9.190	9.377	13.772 (*13.953*)
	d	4.595	4.689	4.591 (*4.651*)
	C–C (×3)	1.447	1.444	1.445
	La–C (×12)	2.75	2.77	2.71
NdC_6	*E*	10	0	3
	a	4.339	4.335 (*4.29*)[b]	4.341 (*4.38*)[a]
	c	9.311	9.431 (*9.37*)	13.925 (*14.41*)
	d	4.656	4.716 (*4.685*)	4.664 (*4.80*)
	C–C (×3)	1.446	1.445	1.447
	La–C (×12)	2.84	2.81	2.74
EuC_6	*E*	5	0	11
	a	4.335	4.332 (*4.314*)[c]	4.334
	c	9.637	9.644 (*9.745*)	14.453
	d	4.819	4.822 (*4.873*)	4.818
	C–C (×3)	1.445	1.444	1.445
	La–C (×12)	2.84	2.81	2.81
YbC_6	*E*	0	3	9
	a	4.333	4.340 (*4.320*)[c] (*4.30*)[b]	4.331
	c	9.270	9.075 (*9.147*)[c] (*9.34*)[b]	13.821
	d	4.633	4.538 (*4.574*)[c] (*4.67*)[b]	4.607
	C–C (×3)	1.444	1.447	1.444
	La–C (×12)	2.74	2.69	2.69
graphite	*a*	4.2758	4.2758	
	c	6.7079	6.7079	
	C–C	1.425 (*1.42*)[16]	1.425 (*1.42*)[b]	

Table 1. Relative cohesive energies *E* (meV per f. u.), computed lattice parameters *a* and *c*, distances between carbon layers *d* (all in Å), and C–C and *Ln*–C bond lengths (Å) (multiplicity in parentheses) for rare earth metal GIC's with different metals and different arrangements (see text). The experimental cell parameters are given in italics when available.

[a] Ref. [19]; [b] ref. [16]; [c] ref. [13].

and the augmentation cut-off energy was about 850 eV. Convergence of the total energy with the number of *k* points and the plane-wave cut-off was checked with an accuracy < 1 meV atom^{-1}.

Results and Discussion

Solid state structure of LnC_6

The three geometries $P6_3(1)$, $P6_3(2)$, and $R3$ with different rare earth metals (*Ln* = La, Ce, Nd, Eu, and Yb) were first optimized. Table 1 lists the results of the corresponding first-principles total energy calculations. With La and Ce, the hexagonal arrangement $P6_3(2)$ is substantially energetically preferred over the other hexagonal $P6_3(1)$ one and the rhombohedral $R3$ one (18 and 40 meV per formula unit (f. u.) for La, and 53 and 68 meV per f. u. for Ce, respectively). Surprisingly, the energy difference is less pronounced with the other metals, Nd, Eu, and Yb. Indeed, the three structural arrangements are nearly isoenergetic (energy difference less than 10 meV) with a very slight preference for the $P6_3(2)$ structure in the case of Nd and Eu, and for the $P6_3(1)$ structure in the case of Yb. These results are not in full agreement with the experimental data since CeC_6 seems to adopt the rhombohedral $R3$ arrangement [19] and YbC_6 the hexagonal $P6_3(2)$ structure [16]. On the other hand, theory and experiment agree on the hexagonal $P6_3(2)$ arrangement for EuC_6. Finally, for NdC_6, experiments propose either the hexagonal $P6_3(2)$ structure [16] or the rhombohedral $R3$ structure [19]. Less than 3 meV per f. u. separate these two arrangements according to our calculations. We cannot exclude that both arrangements exist. Interestingly, the preferred arrangement does not seem to be governed by the usual oxidation states of the rare earth elements (Eu^{2+}, Yb^{2+}, La^{3+}, Ce^{3+} and Nd^{3+}) since for instance the hexagonal $P6_3(2)$ structure is observed for both Eu or La and Ce for instance.

Regardless of the nature of the metals and the structural arrangements, computations give similar cell parameters a of *ca.* 4.33 – 4.34 Å (Table 1), indicating that this cell parameter is mainly determined by the C–C bonds in the carbon sheets. On the other hand, the distance d between carbon sheets depends not only on the size of the metal atoms, but also on the atomic arrangements. This is especially the case for LaC_6, where d is much shorter in the $R3$ structure (4.524 Å) than in the $P6_3(1)$ and $P6_3(2)$ structures (4.818 and 4.884 Å, respectively). The difference is less pronounced for the other GIC's for which d is comparable in the $P6_3(1)$ and $R3$ structures and somewhat smaller than in the $P6_3(2)$ structure in general (Table 1). The experimental structural cell parameters available for a few LnC_6 compounds are also given in Table 1. Their poor accuracy prevents a detailed comparison with the computed values. Nevertheless, except for CeC_6 [18], a deviation of *ca.* 1 % is observed between the computed and experimental a and c cell parameters. Similar a cell parameters for all the GIC's are computed for all the compounds (Table 1). As expected, the C–C bond lengths in GIC's are somewhat longer than that in pristine graphite for which the distance is computed to be 1.425 Å. This is due to some partial filling of the π^*-type bands as a result of the electron transfer from the rare earth metals to the graphite layers (*vide infra*).

Electronic structure of LaC_6

Let us continue with the analysis of the electronic structure of the rare earth metal GIC's. Results being comparable for all the rare earth metals, only those obtained for the three possible arrangements of LaC_6 are presented and discussed here. For a further comparison, the electronic structure of 2D pristine graphite was first considered. The density of states (DOS) of one carbon layer is shown at the top of Fig. 2. As expected, a pseudo-gap at the Fermi level separates the bonding π bands from the antibonding π^* bands [27]. What happens when the La atoms are intercalated in graphite? The DOS for the three arrangements are shown in Fig. 2. They look very similar with the Fermi level crossing a rather high peak of states mainly derived from carbon states with some La $5d$ state admixture. As expected, a narrow La $4f$ DOS peak is found *ca.* 2.5 eV above the Fermi level. Interestingly, rather disperse peaks deriving from the semi-core La $5p$ states at low energy (*ca.* −17 eV) and from the La $5d$ states in the Fermi level energy region are observed

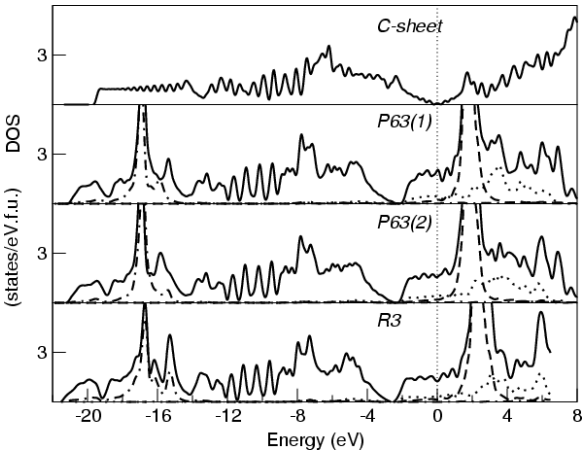

Fig. 2. Total DOS of a graphite sheet (top) and partial and total DOS of LaC_6 with different arrangements (bottom). The filled lines represent the total DOS, dotted lines the La $5d$ states and broken lines La $4f$ characters.

in the DOS. This indicates some covalent interactions between the La and C atoms. A pseudo-gap of about 0.5 eV is found at about 2.5 eV below the Fermi level for the three arrangements (Fig. 2). This pseudo-gap separates the carbon bonding π and antibonding π^* states. These results are in a very good agreement with angle-resolved valence band photoemission spectra of La GIC prepared by a thermally induced surface reaction of a metallic La film on a graphite (0001) substrate [20, 28, 29]. A pseudo-gap of *ca.* 1 eV width is found about 1.5 eV below the Fermi level. Consequently, a partial filling of the carbon antibonding π^* band occurs and leads to C–C bond distances longer than in graphite (*vide supra*).

Indeed, integration of electron density with a Wigner-Seitz sphere of 1.8 Å for La (its covalent radius) gives about 1.1 electrons in the La $5d$ orbitals. Thus, this seems to indicate that La must act roughly as a two-electron donor in LaC_6. In other words, 0.316 electrons are transferred to each carbon atom. This value is very high and is somewhat arbitrary. It must be taken with caution since the atomic integrated electron densities are strongly dependent on the sphere sizes of the ions. Choosing a smaller Wigner-Seitz sphere of 1.5 Å for La for instance (a more realistic radius if we assume that La possesses a strong cationic character in LaC_6), gives about 0.7 electrons in the La $5d$ orbitals, *i. e.*, 0.383 electrons are transferred to each C atom. The charge of the C atoms, *i. e.*, the electron transfer to the graphite sheets, can also be estimated using the empirical Pietonero-Strässler [30] or the Brown [31] for-

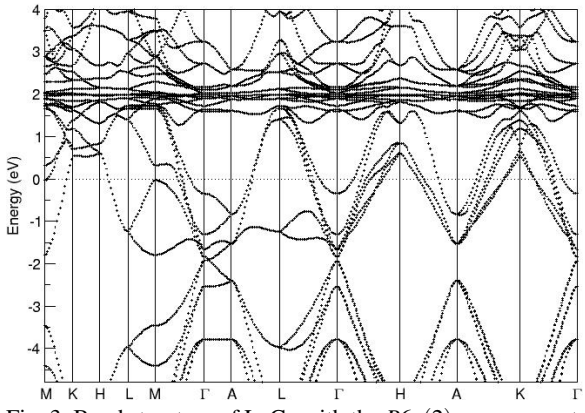

Fig. 3. Band structure of LaC_6 with the $P6_3(2)$ arrangement.

mulae which take into account the C–C bond lengthening in the GIC's with respect to pristine graphite. With an averaged computed C–C bond in LaC_6 of 1.445 Å *vs*. 1.425 Å, the value computed for the graphite sheet (Table 1), the charge transfer is estimated to be about 0.125 (Pietonero-Strässler formula) and 0.166 (Brown formula) electrons per carbon atom, substantially less than the computed value.

The band structure computed for LaC_6 with the $P6_3(2)$ arrangement is shown in Fig. 3. Similar band structures are computed with the other arrangements. Anisotropy is expected for the metallic properties of this GIC. Bands cross the Fermi level along symmetry lines of the hexagonal Brillouin zone (M-K, H-L, M-K, A-L, *etc*.) which correspond to the *a* and *b* axis (carbon sheet planes), but not along lines corresponding to the stacking *c* axis (K-H, L-M, A-Γ, *etc*.), leading to cylindrical Fermi surfaces. Nevertheless, some bands are rather dispersive along lines such as L-M which correspond to the stacking axis, indicating substantial covalent character between the carbon sheets and the metals.

Conclusions

Pseudo-potential first-principles calculations have been performed for ground state structures of intercalates LnC_6 (*Ln* = La, Ce, Nd, Eu, and Yb). The EuC_6-type structure ($A\alpha A\beta A\alpha A\beta A\alpha A$ stacking) is energetically slightly preferred for La and Ce, whereas with the other rare earth metals the GIC's have almost the same cohesive energies for the three different atomic arrangements $A\alpha A\alpha A\alpha A\alpha A\alpha A\ldots$, $A\alpha A\beta A\alpha A\beta A\alpha A\ldots$, and $A\alpha A\beta A\gamma A\alpha A\beta A\ldots$ A rather important charge transfer occurs from the metals to the carbon sheets, the electrons partially occupying the bottom of the carbon π^* band. As a consequence, a lengthening of the C–C bonds of *ca*. 0.02 Å is computed with respect to the C–C bond lengths in graphite. Two-dimensional metallic character is expected for LaC_6 as inferred from its band structure.

Acknowledgements

The authors thank the Institut de Développement et de Ressources en Informatique Scientifique (IDRIS-CNRS) and the Centre Informatique National de l'Enseignement Supérieur (CINES) for computing facilities. C.-M. Fang thanks the Centre National de la Recherche Scientifique (France) for a Visiting Scientist fellowship.

[1] M. S. Dresselhaus, G. Dresselhaus, *Adv. Phys*. **1981**, *30*, 139; *ibid*. **2002**, *51*, 1.
[2] N. B. Hannay, T. H. Geballe, B. T. Matthias, K. Andres, P. Schmidt, D. MacNair, *Phys. Rev. Lett*. **1965**, *14*, 225.
[3] P. Bak, *Phys. Rev. Lett*. **1980**, *44*, 889.
[4] N. Emery, C. Hérold, M. d'Ástuto, V. Garcia, Ch. Belin, J. F. Marêché, P. Lagrange, G. Loupias, *Phys. Rev. Lett*. **2005**, *95*, 087003.
[5] D. Guérard, A. Hérold, *C. R. Acad. Sc. Paris*, *Sér. C* **1975**, *t. 280*, 729.
[6] D. Guérard, A. Hérold, *C. R. Acad. Sc. Paris*, *Sér. C* **1974**, *t. 279*, 455.
[7] G. Kainl, J. Feldhaus, U. Ladewig, K. H. Frank, *Phys. Rev. Lett*. **1983**, *50*, 123.
[8] T. E. Weller, M. Ellerby, S. S. Saxena, R. P. Smith, N. T. Skipper, *Nat. Phys*. **2005**, *1*, 39.
[9] G. Csányi, P. B. Littlewood, A. H. Nevidomskyy, C. J. Pickard, B. D. Simons, *Nat. Phys*. **2005**, *1*, 42.
[10] I. I. Mazin, *Phys. Rev. Lett*. **2005**, *95*, 227001.
[11] J. X. Shi, Y. D. Wei, *J. Phys. Chem. Solids* **1999**, *60*, 363.
[12] A. Hérold, *Synthetic Metals* **1988**, *23*, 27.
[13] M. EI Makrini, D. Guérard, P. Lagrange, A. Hérold, *Carbon* **1980**, *18*, 203.
[14] D. Guérard, A. Hérold, *C. R. Acad. Sc. Paris*, *Sér. C* **1975**, *t. 281*, 929.
[15] R. Hagiwara, M. Ito, Y. Ito, *Carbon* **1996**, *34*, 1591.
[16] I. I. Mazin, S. L. Molodtsov, *Phys. Rev*. **2005**, *B72*, 172504.
[17] S. L. Molodtsov, T. Gantz, C. Laubschat, A. G. Viatkine, J. Casado, M. C. Asensio, *Z. Phys*. **1996**, *B100*, 381.
[18] S. L. Molodtsov, F. Schiller, S. Danzenbächer,

M. Richter, J. Avila, C. Laubschat, M. C. Asensio, *Phys. Rev*. **2003**, *B67*, 115105.

[19] J. Bauer, unpublished results. Very thin plates of "CeC_6" were found in an arc-melted and annealed two-phase sample of a nominal composition of 14.5 atom % Ce, 14.5 atom % B and 71 atom % C mixed with the ternary phase CeB_2C_4 (C.-M. Fang, J. Bauer, J.-Y. Saillard, J.-F. Halet, submitted for publication). The lack of reflections which obey the general diffraction conditions $-h+k+l = 3n$ demonstrates rhombohedral symmetry with cell parameters a = 4.490(1) and c = 13.9526(4) Å. The large a parameter with respect to that measured for other LnC_6 GIC's indicates that the "CeC_6" phase must contain a few at. % of boron. Attempts of preparation of the binary phase were unsuccessful. On the other hand, the arc-melted NdC_6 phase was prepared starting from powders of neodymium and carbon. X-Ray powder diffraction data of poor quality were used to propose also the rhombohedral symmetry with lattice parameters a = 4.38(1) and c = 14.41(7) Å.

[20] A. M. Shikin, V. K. Adamchuk, S. Siebentritt, K.-H. Rieder, S. L. Molodtsov, C. Laubschat, *Phys. Rev*. **2000**, *B61*, 7752.

[21] G. Kresse, J. Furthmüller, *Phys. Rev*. **1996**, *B54*, 11169.

[22] G. Kresse, J. Furthmüller, *Comput. Mat. Sci*. **1996**, *6*, 15.

[23] P. E. Blöchl, *Phys. Rev*. **1994**, *B50*, 17953.

[24] G. Kresse, J. Furthmüller, *Phys. Rev*. **1999**, *B54*, 1758.

[25] J. P. Perdew, S. Burke, M. Ernzerhof, *Phys. Rev. Lett*. **1996**, *77*, 3865.

[26] H. J. Monkhorst, J. D. Pack, *Phys. Rev*. **1976**, *B13*, 5188.

[27] R. Ahuja, S. Auluck, J. Trygg, J. M. Wills, O. Eriksson, B. Johansson, *Phys. Rev*. **1995**, *B51*, 4813.

[28] A. M. Shikin, S. L. Molodtsov, C. Laubschat, G. Kaindl, G. V. Prudnikova, V. K. Adamchuk, *Phys. Rev*. **1995**, *B51*, 13586.

[29] S. L. Molodtsov, C. Laubschat, M. Richter, Th. Gantz, A. M. Shikin, *Phys. Rev*. **1996**, *B53*, 16621.

[30] L. Pietronero, S. Strässler, *Phys. Rev. Lett*. **1981**, *47*, 593.

[31] I. D. Brown, *Acta Crystallogr*. **1977**, *B33*, 1305.